IMPULSE PHOTOTHERMAL EVALUATION OF MATERIALS VIA FREQUENCY MODULATED OPTICAL REFLECTANCE I: THEORY

A. Mandelis and J.F. Power

Photoacoustic and Photothermal Sciences Laboratory
Department of Mechanical Engineering
University of Toronto
5 King's College Road
Toronto, Ontario
M5S 1A4 Canada

INTRODUCTION

Recently, laser induced thermal wave based technologies have provided a powerful class of techniques for the evaluation of solid state materials [1,2]. Through the use of tightly focussed optical beams modulated at high frequencies, it has been possible to both generate and interrogate highly localized thermal wave phenomena in materials with spatial resolutions approaching 1 μm [2]. The unique capability for thermal depth profiling of optically opaque materials is possible with surface thermal wave measurements because of the rather obvious relationship between the vertical depth of a buried feature and the transit time of thermal energy to the sample surface.

Photothermal techniques which use impulse irradiation [3,4] yield an important advantage over methods which use single frequency CW modulation, since an impulse measurement enables a direct, time visualization of thermal energy arriving at the sample surface from buried subsurface layers. In this work, we derive a three dimensional Green's function model for the thermal response of a sample excited by a tightly focussed beam of radiation. The theory provides analytical time-domain expressions for the thermal pulse propagation in homogeneous solids and thin surface layers and is expected to be generally useful in both quantitative thermal evaluation and imaging applications with well characterized geometries. The theory presented in this section is applied to the interpretation of the experimental results of Part II of this work, in which we have utilized a powerful technique of thermally modulated optical reflectance [1,3] to extract fast, high quality impulse response information from some well characterized materials, using a novel frequency modulation technique [5].

GENERAL THEORY OF THE THREE DIMENSIONAL PHOTOTHERMAL GREEN'S FUNCTION IN SOLIDS

The detection of thermal wave propagation in materials by optical reflectance involves thermally induced changes in the sample's surface optical reflectivity according to the reflectivity response [6]:

$$\Delta R(r,z=0,t) = R_0 + \left[\frac{\partial R}{\partial T}\right]_{T=0} \Delta T_2(r,z=0,t) \tag{1}$$

where R_0 is the surface reflectivity of the sample at ambient temperature, and $\partial R/\partial T$ is the temperature coefficient of surface reflectance.

The temperature distribution in the sample $T_2(r,z,t)$ was obtained from the solution, in cylindrical coordinates, of the homogeneous heat conduction equation in the form (see Fig. 1):

$$\nabla^2 T_i(r,z,t) - \frac{1}{\alpha_i}\frac{\partial T(r,z,t)}{\partial t} = 0$$

assuming continuity of heat flux and temperature at each of the interfaces. By means of the Sommerfeld Hankel transform method [7] it was possible to evaluate the Laplace transform of the thermal response in each of the three layers in terms of the closed form expressions:

$$\bar{T}_1(r,z,s) = \int_0^\infty J_0(kr)\, A(k)\, e^{-\sigma_1 z}\, dk \quad ; \quad z \geq 0 \tag{2a}$$

$$\bar{T}_2(r,z,s) = \int_0^\infty J_0(kr) \left[C(k)\, e^{\sigma_2 z} + D(k)\, e^{-\sigma_2 z} + \frac{k e^{-\sigma_2 |z|}}{4\pi\alpha_2\sigma_2} \right] dk \quad ; \quad 0 \geq z \geq -l \tag{2b}$$

$$\bar{T}_3(r,z,s) = \int_0^\infty J_0(kr)\, B(k)\, e^{\sigma_3(z+l)}\, dk \quad ; \quad z \leq -l \tag{2c}$$

where A, B, C, and D are coefficients, evaluated at the boundaries. The σ_i variable is a thermal wavenumber given as follows:

$$\sigma_i(s) = [k^2 + q_i^2(s)]^{1/2} \tag{3}$$

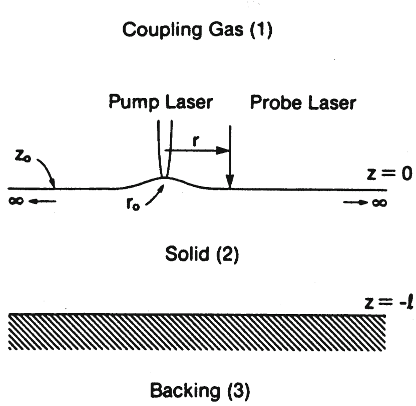

Fig. 1 Three dimensional geometry for thermal impulse response (Green's function) of sample to point irradiation.

Analytical inversions of Eq. (2) have been obtained for special cases of experimental interest and are reported below.

SPECIAL CASES

I. The Semi-infinite Solid

In the limit of a semi-infinite solid ($l \to \infty$), with zero heat flux at the gas/sample interface, the experimental surface temperature, derived from the inversion of Eq. (2) is given as:

$$T_1(r,0,t) = \frac{1}{4(\pi\alpha_2 t)^{3/2}} e^{-r^2/4\alpha_2 t} \tag{4}$$

The effect of the finite cross section of the irradiating beam was incorporated into the model by convolution of the pump beam's TEM(0,0) intensity distribution with the radial part of the Green's function in Eq. (4). The resulting expression for the semi-infinite sample was:

$$T_1(r,0,t) = \frac{P_0 w_0^2}{2\pi(\pi\alpha_2 t)^{1/2}(4\alpha_2 t + w_0^2)} e^{-r^2/(4\alpha_2 t + w_0^2)} \tag{5}$$

and shows a transition from three dimensional to one dimensional behavior as the irradiation spot size is increased to large values: $w_0^2 \gg 4\alpha_2 t$.

The semi-infinite response contains no depth profiling information but provides a useful single ended method for the measurement of the sample's bulk thermal diffusivity. By monitoring the thermoreflectance signal at various offset positions from the pump beam center one obtains a thermal response of the form: $A\, t^{-3/2}\, e^{-r^2/4\alpha_2 t}$ yielding an impulse response profile with a well defined maximum at $\tau_d = r^2/6\alpha_2$ due to the finite time for the transit of thermal energy to the offset position, r (Fig. 2). Note that all of the thermal responses in the figure have been normalized to unity peak value.

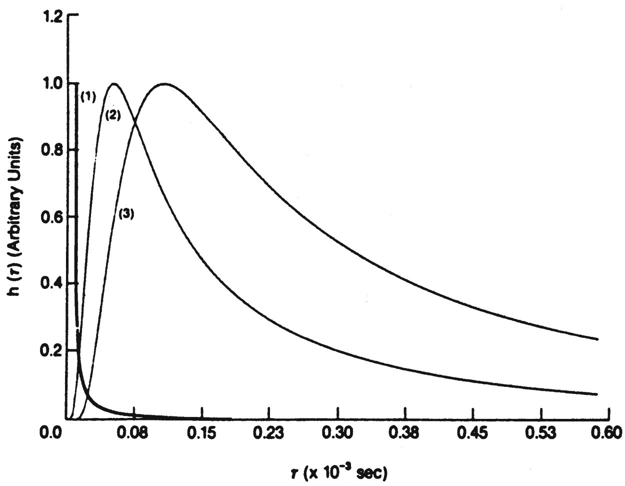

Fig. 2 Impulse response (Green's function) for a three dimensional semi-infinite solid sample, at probe beam offset distances, $r = 0.1\ \mu m$ (1); $4\ \mu m$ (2); and $6\ \mu m$ (3). $\alpha_2 = 6\times10^{-8}\ m^2/s$.

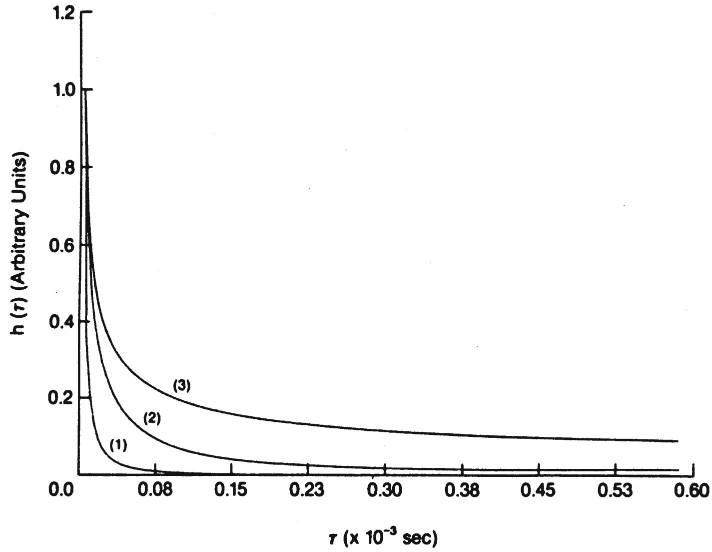

Fig. 3 Impulse response (Green's function) for three dimensional semi-infinite solid sample with $\alpha_2 = 5\times10^{-7}\ m^2/s$ and pump beam waist size w_0 = 1 μm (1); 10 μm (2); and 1 mm (3).

II. Conducting Thin Layer with Insulating Boundaries

The impulse response of a conducting thin layer with adiabatic boundaries (gas/sample and sample/backing) is derived from Eqs. 2a-c to give the following result:

$$T_1(r,0,t) = \frac{e^{-r^2/4\alpha_2 t}}{4(\pi\alpha_2 t)^{3/2}} \sum_{n=0}^{\infty} \left[e^{-(2nl)^2/4\alpha_2 t} + e^{-[2(n+1)l]^2/4\alpha_2 t} \right] \tag{6}$$

When the radial part of Eq. (6) is convoluted with the pump beam's intensity profile, the resulting dependence on w_0 is identical to Eq. (4). As in the semi-infinite case, a transition from three to one dimensional heat conduction is observed as $w_0{}^2 \gg 4\alpha t$ (Fig. 4).

The number of terms required to bring about convergence of Eq. (6) is directly determined by the number of thermal reflections taking place at the boundaries $z = 0$ and $z = -l$, and may be understood by folding or reflecting the semi-infinite response back into the region $-l < z < 0$ (Fig. 5). This is directly consistent with the Method of Images [8]. The peak response of the sample's temperature profile damps as $t^{-3/2}$ while the variance of the "folded" semi-infinite distribution increases as $\sigma^2 = \mu^2$. The relative depth of penetration of the temperature gradient in the sample, is determined by the time dependent thermal diffusion length $\mu = \sqrt{4\alpha_2 t}$. For a fixed time delay the thermal penetration depth in an insulator will be very shallow, while the corresponding penetration depth in a highly conducting sample such as a metal, will be long range. More terms at earlier time delays are clearly required for convergence of Eq. (5) in the case of highly conducting materials (Fig. 6). At very early times past excitation, the surface temperature obeys the semi-infinite response because a negligible amount of thermal energy reaches the substrate layer until $\tau \approx l^2/4\alpha$. This explains the convergence of all of the impulse response profiles predicted for a wide range of α values, to a common response at the earliest times. These results are consistent with similar physical trends, both theoretical and experimental, reported earlier using pulsed photothermal radiometry [4].

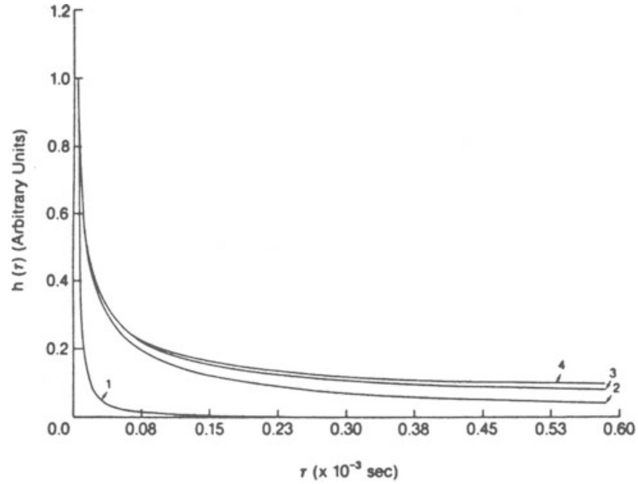

Fig. 4 Theoretical predictions of the 3D to 1D transition in the impulse response of a 9 μm thick insulator ($\alpha_2 = 6\times10^{-8}\ m^2/s$) as a function of beamwaist size. Probe beam offset position $r = 0.1\ \mu m$ from the center of the pump beam. w_0 values were 0.1 μm (1); 10 μm (2); 25 μm (3); and 100 μm (4).

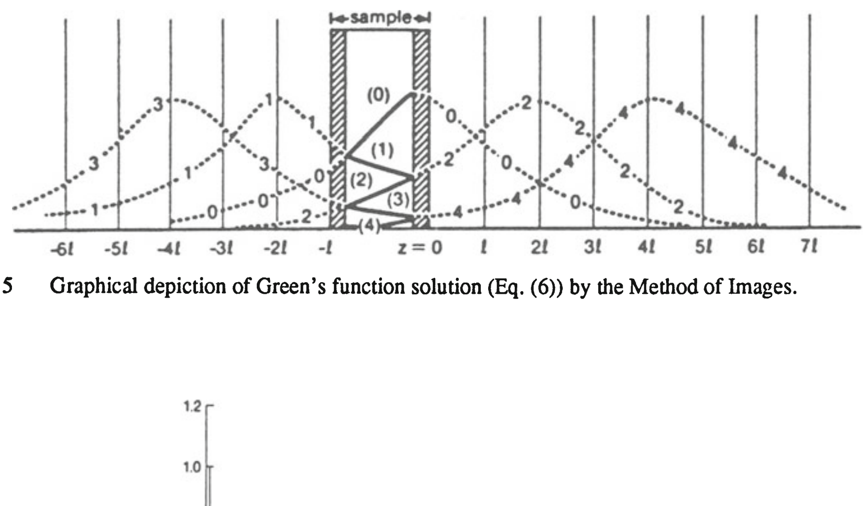

Fig. 5 Graphical depiction of Green's function solution (Eq. (6)) by the Method of Images.

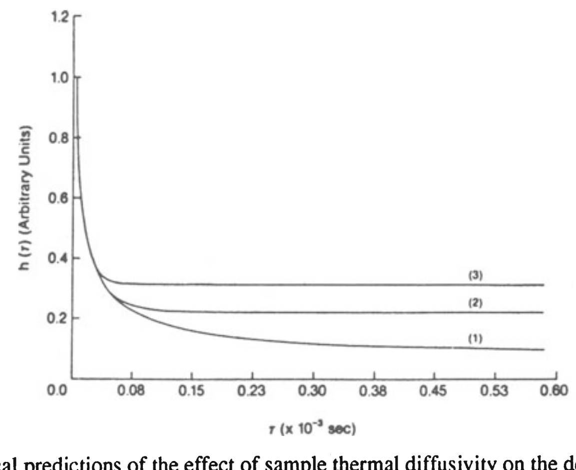

Fig. 6 Theoretical predictions of the effect of sample thermal diffusivity on the decay profile of the one dimensional temperature field. $\alpha_2 = 8\times10^{-8}\ m^2/s$ (1); $4\times10^{-7}\ m^2/s$ (2); and $8\times10^{-7}\ m^2/s$ (3). Other parameters are $r = 0.1\ \mu m$; $l = 20\ \mu m$; $w_0 = 1\ mm$; n = 100.

III. Detection of Buried Heat Sinks

The expression for the thermal Green's function in a sample layer with a thermally conducting backing as derived from Eq. 2a-c is given below:

$$T_2(r,z,t) = \frac{e^{-r^2/4\alpha_2 t}}{8(\pi\alpha_2 t)^{3/2}} (e^{-z^2/4\alpha_2 t}$$

$$+ \sum_{n=0}^{\infty}(-1)^n [e^{-(2nl-z)^2/4\alpha_2 t} - e^{-[2(n+1)l-z]^2/4\alpha_2 t} - 2e^{-[2(n+1)l+z]^2/4\alpha_2 t}]) \qquad (7)$$

Beam profile effects were incorporated as in the previous two cases. The effect of sample thickness on the surface impulse response profile is explored in Fig. (7). The top curve is the typical one dimensional response predicted for a sample in which the thermal profile is attenuated before much of the energy reaches $z = -l$. A heat sink placed at $z = -l$ has very little effect on the thermal decay profile in this range. As the heat sink is moved closer to the front surface, the surface thermal impulse profile slopes downward until effectively the entire temperature profile is damped within approximately 10 thermal transit times. The effect is quite pronounced with very thin samples.

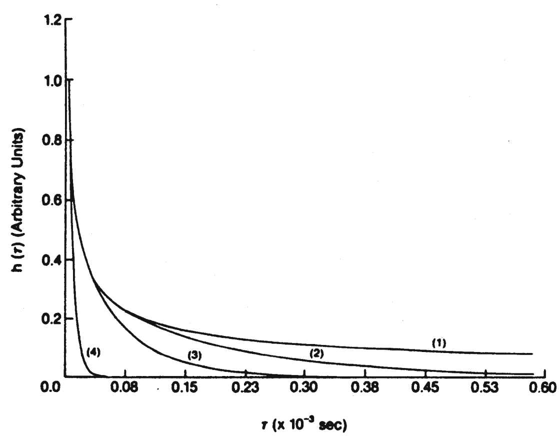

Fig. 7 One dimensional theoretical predictions of the effect of the presence of a heat sink in contact with a solid of variable thickness. Sample thickness: l = 100 μm (1); 5 μm (2); 3 μm (3); and 1 μm (4). Other parameters are $r = 1\times10^{-7}$ m; $w_0 = 1$ mm; $\alpha_2 = 6\times10^{-8}$ m^2/s; n = 100.

REFERENCES

1. A. Rosencwaig, J. Opsal, W.L. Smith, and D.L. Willenborg, Appl. Phys. Lett. **46**, 1013 (1985).
2. J. Opsal, A. Rosencwaig, and D.L.Willenborg, Appl. Opt. **22**, 3169 (1983).
3. C.A. Paddock and G.L. Eesley, J. Appl. Phys. **60**, 285 (1986).
4. A. Tam in *Photoacoustic and Thermal Wave Phenomena in Semiconductors*, A. Mandelis Ed. (North-Holland, New York, 1987) Ch. 8.
5. A. Mandelis, I.E.E.E. Trans. U.F.F.C. **UFFC-33**, 590 (1986).
6. M. Cardona, *Modulation Spectroscopy* (Academic, New York 1969) pp. 117-136.
7. A. Sommerfeld, Ann. Physik **28**, 665 (1909) and J. Stratton, *Electromagnetic Theory* (McGraw Hill, New York, 1984) pg. 573.
8. P.M. Morse and H. Feshbach, *Methods of Theoretical Physics* (McGraw-Hill, New York, 1953) pg. 812.